Qualitative EEG abnormalities signal a shift towards inhibition-dominated brain networks. Results from the EU-AIMS LEAP studies

Erika L. Juarez-Martinez[1,2], Arthur-Ervin Avramiea[1,2], Pilar Garcés[3], Joerg F. Hipp[3], Simon-Shlomo Poil[4], Marina Diachenko[1], Huibert D. Mansvelder[1], Emily Jones[5], Luke Mason[6], Declan Murphy[6,7], Eva Loth[6], Bethany Oakley[6], Tony Charman[8], Tobias Banaschewski[9], Bob Oranje[10], Jan Buitelaar[11], Hilgo Bruining[2,12,13†*], Klaus Linkenkaer-Hansen[1†*]

[†]These authors contributed equally to this work.

Abstract

Qualitative EEG abnormalities are common in Autism Spectrum Disorder (ASD) and hypothesized to reflect disrupted excitation/inhibition balance. To test this, we recently introduced a functional measure of network-level E/I ratio (fE/I). Here, we applied fE/I and other quantitative EEG measures to alpha oscillations from source-reconstructed data in the EU-AIMS compilation of 267 EEG recordings from children-adolescents and adults with ASD and 209 controls. We analyzed these quantitative measures alongside evaluating for qualitative EEG abnormalities ranging from slowing of activity to epileptiform patterns aiming to replicate the findings from the SPACE-BAMBI study (Bruining et al., 2020). EEG abnormalities were only identified in a few adults and could not be statistically assessed. ASD children-adolescents with EEG abnormalities exhibited lower relative alpha power and lower fE/I compared to children-adolescents without abnormalities; however, the EEG-abnormality scoring did not stratify the behavioral heterogeneity of ASD using clinical measures. Surprisingly, several controls presented with qualitative EEG abnormalities and showed a strikingly similar anatomical distribution of lower fE/I to the one observed in the ASD group, suggesting a shift towards inhibition-dominated network dynamics, in regions associated with altered sensory processing. The robustness of this association between EEG abnormalities and reduced fE/I was further supported by re-analysis of the SPACE-BAMBI study in source space. Stratification by the presence of EEG abnormalities and their associated effects on network activity may help understand neurodevelopmental

physiological heterogeneity and the difficulties in implementing E/I targeting treatments in unselected cohorts.

Author affiliations:

[1]Department of Integrative Neurophysiology, Center for Neurogenomics and Cognitive Research, (CNCR), Amsterdam, Neuroscience, VU Amsterdam, 1081 HV Amsterdam, The Netherlands.

[2]Child and Adolescent Psychiatry and Psychosocial Care, Emma Children's Hospital, Amsterdam UMC, Vrije Universiteit Amsterdam, Meibergdreef 5, 1105 AZ, Amsterdam, The Netherlands.

[3]Roche Pharma Research and Early Development, Neuroscience and Rare Diseases, Roche Innovation Center Basel, Basel, Switzerland.

[4]Aspect Neuroprofiles BV, Amsterdam, The Netherlands.

[5]Department of Psychological Sciences, Centre for Brain and Cognitive Development, Birkbeck, University of London, London, UK.

[6]Department of Forensic and Neurodevelopmental Sciences, Institute of Psychiatry, Psychology and Neuroscience, King's College London, UK.

[7]Institute for Translational Neurodevelopment/ South London and Maudsley NHS Foundation Trust.

[8]Department of Psychology, Institute of Psychiatry, Psychology and Neuroscience, King's College London, UK.

[9]Department of Child and Adolescent Psychiatry and Psychotherapy, Central Institute of Mental Health, Medical Faculty Mannheim, University of Heidelberg, German Center for Mental Health (DZPG), partner site Mannheim-Heidelberg-Ulm, Mannheim, Germany.

[10]Center for Neuropsychiatric Schizophrenia Research (CNSR), Copenhagen University Hospital, Psychiatric Center Glostrup, Denmark.

[11]Department of Cognitive Neuroscience, Donders Institute for Brain, Cognition and Behaviour, Radboudumc, Nijmegen, The Netherlands.

[12]N=You Neurodevelopmental Precision Center, Amsterdam Neuroscience, Amsterdam Reproduction and Development, Amsterdam UMC, Amsterdam, The Netherlands.

[13]Levvel, Center for Child and Adolescent Psychiatry, Amsterdam, The Netherlands.

Correspondence to: Klaus Linkenkaer-Hansen

Full address: De Boelelaan 1085, 1081 HV Amsterdam, The Netherlands

E-mail: klaus.linkenkaer@cncr.vu.nl

Correspondence to: Hilgo Bruining

Full address: Meibergdreef 9 1105 AZ Amsterdam

E-mail: h.bruining@amsterdamumc.nl

Running title: EEG abnormalities reflect inhibition

Keywords: Autism spectrum disorder, EEG, excitation-inhibition balance

Introduction

The opposing forces of excitation (E) and inhibition (I) fundamentally shape activity at many levels of neuronal organization. Heuristic arguments have favored a certain balance in E/I ratios to be important for normal brain function[1], which has been underscored by a large body of computational modeling in recent years[2–5]. Disturbances in E/I ratios at various levels of neuroscientific interrogation have been associated with autism spectrum disorder (ASD)[6–17], among other disorders[18]. The original implication of E/I imbalances in ASD was based upon its high comorbidity with epilepsy and the frequently observed EEG abnormalities (ranging from epileptiform patterns to non-epileptiform activity such as slowing)[19–22]. Preclinical support for the E/I imbalance theory ranges from genetic studies on synaptic proteins to postmortem analyses of GABAergic and glutamatergic systems[11,12,23–25]. Collectively, the results indicate that up and down regulation of both excitation and inhibition may contribute to ASD manifestations, probably reflecting a mixture of primary and secondary interactions around homeostatic mechanisms[25]. Thus, variation in E/I directionality within ASD may result in different forms of pathophysiology and, in turn, variability in treatment response[17,24,25].

An important challenge is to develop clinically-applicable methods to increase our understanding of global network E/I imbalances in addition to the knowledge gained at the local or cellular level. In vivo, markers of E/I balance are being developed, e.g., using magnetic resonance spectroscopy, which can quantify concentrations of inhibitory (GABA) and excitatory (glutamate) neurotransmitters[13–17]. Although promising, these studies are hampered by the limited spatial and temporal resolution. More recently, quantitative EEG techniques have been proposed as proxy markers for E/I balance in mass brain activity[26]. Our

group has put forward a definition of network E/I balance that is inspired by computational modeling of critical brain dynamics[27,28]. In this framework, E/I balance is an emergent network property—characterized by high spatio-temporal complexity emerging in neuronal networks balancing between order and disorder. This definition enables measuring a network-level functional E/I ratio (fE/I), which is useful for understanding basic principles of information processing in neuronal networks[2–4,29–31] and for studying brain disorders in which E/I balance may be disrupted. The fE/I method has shown sensitivity to changes in both network connectivity and synapse functioning through simulations[3]. Importantly, it is directly applicable to EEG recordings, making it well-suited for clinical use. Indeed, fE/I estimation in EEG recordings corresponding to a large sample of healthy controls, confirmed an overall balanced network E/I ratio. We further validated the method using pharmacological manipulation in healthy subjects with a GABAergic drug[27].

In parallel, our group investigated network-level fE/I for the first time in a clinical population of children with ASD[27]. In line with the aforementioned findings from preclinical studies, we found that ASD is characterized by both increased and decreased E/I ratios supporting the notion that E/I variability is substantial. Importantly, we found a strong association between qualitative EEG abnormalities identified through visual inspection and fE/I variability, supporting the hypothesis that epileptiform activity and EEG abnormalities relate to E/I imbalances. Furthermore, we implemented fE/I in an innovative randomized controlled trial testing bumetanide as an E/I targeting treatment and confirmed that the measure is treatment sensitive[32]. These findings provide an initial proof-of-concept of the utility of fE/I estimation for physiological stratification in ASD[27].

Based on these initial observations, we hypothesize that establishing an association between qualitative and quantitative EEG abnormalities in ASD is instrumental to understand the implication of E/I imbalances towards network and information processing dysfunctions. In this line, fE/I estimation comes to light as an appropriate measure to study the diverse network-level E/I dynamics that may result from primary pathophysiological mechanisms or compensatory mechanisms that counteract epileptogenic activity. Here, we elaborated on these hypotheses and investigated fE/I variability in the large EU-AIMS compilation of EEG recordings in children-adolescents and adult samples with or without ASD. We make three predictions: first, that the EU-AIMS dataset reproduces the increased variability in fE/I observed in ASD when compared to controls[27]; second, that qualitative EEG abnormalities

are associated with alterations in network E/I as reported in[27]; and third, that the presence of qualitative EEG abnormalities modulates the effect of network E/I on clinical outcome.

Materials and methods

Participants

EU-AIMS

Participants aged 6 to 32 years were recruited between January 2014 and March 2017 across five European specialist ASD centers and their EEG data collected as part of the EU-AIMS Longitudinal European Autism Project (LEAP). A complete description of the study design and clinical characterization of the participants can be found in[33,34]. Inclusion criteria for the ASD sample were an existing clinical diagnosis of ASD according to the DSM-IV[35], DSM-IV-TR, DSM-5[36], or ICD-10[37] criteria. ASD symptoms were additionally assessed using the Autism Diagnostic Observation Schedule (ADOS[38,39]) and the Autism Diagnostic Interview-Revised (ADI-R[40]). However, individuals with a clinical ASD diagnosis who did not reach cut-offs on these instruments were not excluded. Psychiatric conditions (except for psychosis or bipolar disorder) and medication use were allowed. Exclusion criteria for the control sample were a T score of $\geq$ 70 on the self-report or parent-report form of the Social Responsiveness Scale[41], presence of any psychiatric disorder and/or psychoactive medication use, and a total IQ <75 (Intellectual disability). For the ASD sample in this study, an IQ < 50 was an exclusion criteria to include a wide range of the ASD spectrum but also limit it to the criteria used in the earlier study that we aim to replicate[27]. The clinical scales included were the Repetitive Behavior Scale-Revised (RBS-R; total raw score; range 0−129, higher score indicates more affected)[42] and the Vineland-II Adaptive Behavior standard score (VABS[43]). The latter assess the adaptive behavior grouped into four major domains: Communication, Daily living, Socialization and Motor skills (VABS-com, VABS-dl and VABS-soc respectively). Sums of the scores from these domains are standardized, higher scores indicate better adaptive behavior (range 86–100) and lower scores indicate low adaptive behavior (<85). Finally, the sums of the domain standard scores are further standardized into an Adaptive Behavior Composite Score (VABS-composite). The study was approved by the

medical ethical committee at each site independently. All participants or their legal guardians signed informed consent.

SPACE-BAMBI

EEGs and symptom-scale baseline measurements were collected from two ongoing studies at the developmental disorder unit in the UMC Utrecht, with identical EEG measurement protocols (SPACE (Sensory information Processing in Autism and Childhood Epilepsy) and BAMBI (Bumetanide in Autism Medication and Biomarker, Eudra-CT 2014-001560-35)). Inclusion criteria for ASD and TDC samples were an age between 7–16 years, IQ > 55, and ability to comply with study procedures. ASD diagnosis required an expert diagnosis according to the Diagnostic and structural manual of mental disorders (DSM) IV-TR[35] or 5[36] supported by a clinical score on the Autism Diagnostic Observation Schedule 2 (ADOS-2 module 3 or 4, score ≥ 7) or a subclinical score on the Social Responsivity Scale (SRS-t-score ≥ 60)[44]. An abbreviated form of the Wechsler intelligence scale for children (WISC)-III was used for IQ estimation. Exclusion criteria for the ASD sample were use of psychoactive medication and presence of other major neurological disease such as previous or current epilepsy diagnoses. The TDC sample was recruited from local residents attending non-special education, where a history of behavioral or learning problems, a diagnosis of any neurodevelopmental condition or any other major health issue was an exclusion criterion.

We recruited a total of 126 subjects that met the inclusion criteria for ASD and 37 TDC. From these, 26 children-adolescents with ASD and 8 TDC were excluded because less than 50% of their recordings were free of transient artifacts or no eyes-closed rest EEG had been recorded. Thus, the final included sample consisted of 129 subjects (42 females): 100 with ASD (7–16 years, M = 10.5 years, SD = 2.3 years, 27 females) and 29 age-matched typically developing children-adolescents (TDC) (7.4–14.4 years, M = 10.3, SD = 1.5 years, 15 females). The study was approved by the medical ethical committee. All participants or their legal guardians signed informed consent.

EEG recordings and pre-processing

EU-AIMS

EEGs were recorded during 4 minutes of resting state per participant (2 min eyes open, 2 min eyes closed) in five different centers: Central Institute of Mental Health (CIMH, Mannheim, Germany), Institute of Psychiatry, Psychology and Neuroscience, King's College London (KCL, UK), Radboud University Nijmegen Medical Centre (RUNMC, Netherlands), University Campus BioMedico (UCBM, Rome, Italy) and University Medical Centre Utrecht (UMCU, Netherlands). The following EEG systems were employed: Brain Vision (CIMH, KCL, RUNMC), BioSemi (UMCU) and Micromed (UCBM), with sampling frequencies of 5000 Hz (KCL, RUNMC), 2048 Hz (UMCU), 2000 Hz (CIMH) and 256–1000 Hz (UCBM). All sites used 10-20 layout caps, with 60–64 electrodes. To optimize participant compliance, resting state was acquired in 30 sec blocks, alternating eyes open (fixating an hourglass) and eyes closed. Segments were then concatenated into a single signal for each condition. To simplify our analysis and in accordance with Bruining *et al.*[27], only the eyes-closed condition was analyzed for this study, since, in children, ECR is less prone to movement and other artifacts. Researchers were blind to group label and the clinical characteristics of the participants (other than age) until after the EEG analysis was carried out (Neurophysiological Biomarker Toolbox and custom-made scripts[45]). Data were homogenized by selecting 61 common electrodes (data from outer electrodes FT9, FT10, TP9, TP10, P9, P10, PO9, PO10 and Iz, if recorded, was discarded, since these electrodes were often noisy or not standard in all the samples), resampled to 1000 Hz and band-pass filtered to 1–32 Hz with a finite impulse response filter. Artifact rejection was performed manually: we eliminated the bad channels and then discarded noisy intervals, after which we re-referenced to the average reference. EEGs were considered of sufficiently good quality to reliably estimate temporal and excitation-inhibition ratio biomarkers (i.e., DFA and *fE/I*), if they contained enough noise-free segments of $\geq$2 seconds to add up to at least 80 seconds of data. Following this criteria, 63 recordings were excluded from analysis (control group: n = 19, ASD group: n = 44; **Figure 1**). After pre-processing, on average 108 seconds per recording (84–131 s) were available for analysis for the ASD group. For the control group on average 110.3 seconds per recording (80–132 s) were available for analysis.

SPACE-BAMBI

EEGs were recorded during 3–5 minutes of eyes-closed rest at the UMC Utrecht using A 64-

channel BioSemi EEG system at a sampling rate of 2048 Hz and common mode sense (CMS) reference electrode.

EEG analyses were initially pre-processed using the in-house developed Neurophysiological Biomarker Toolbox (NBT) written in MATLAB. All recordings were manually cleaned for artifacts, i.e., noisy channels were discarded and noisy intervals removed. Subsequently, the data were re-referenced to the average reference. An average of 217 seconds (range 61–308 s) per recording were available for analysis for the children with ASD and TDC samples.

EEG source localization

We used L2 minimum norm estimation, as implemented by MNE-Python, to obtain cortical current estimates from our sensor level data. The FreeSurfer average brain template from FreeSurfer 6[46] was used to construct the boundary element head model and forward operator for the source modelling. The regularization parameter was set to $\lambda^2 = 1/9$. A diagonal matrix with 0.2 V values was used for the covariance matrix, which was the default values for EEG provided by MNE-Python. Unconstrained orientations were allowed, and principal component analysis was employed on the whole source time series at each vertex to reduce the three-dimensional signals to one-dimensional time series of the dominant principal component. The time series of the 20484 source vertices were further collapsed into 68 cortical patches based on the Desikan Killiany atlas, by first aligning the dipole orientations by shifting vertices with opposite polarity to the majority of vertices by π, followed by averaging the amplitudes of all vertices within a patch. The phase shifting prevents the vertices with opposite polarities from canceling each other out during the averaging operation. Some of the estimated EEG features were computed across cortical brain regions, i.e., patches within frontal, parietal, temporal, occipital, cingulate, and insular regions were averaged. The individual patches were mapped to the brain regions according to the appendix in Klein *et al.*[47].

EEG analysis

We focused our analysis on alpha-band oscillations (8–13 Hz) due to their relevance for healthy neuronal network development and cognitive function[48], their clear disruption in neurodevelopmental disorders, but also to reduce the number of comparisons[49,50].

Power

Spectral power was computed using multitaper spectral estimation[51]. Relative alpha power is expressed in percent and was calculated by dividing the absolute power in the alpha band with the integrated power in the range of 1–45 Hz.

Temporal structure

Neuronal oscillations exhibit complex fluctuations in amplitude that are characterized by a power-law decay of auto-correlations, also known as LRTC[52]. Computational modeling has shown that the strength of LRTC is influenced by the balance between excitatory and inhibitory signaling in the network producing the oscillations[28]. We used the detrended fluctuation analysis (DFA) to quantify LRTC in the amplitude modulation of alpha oscillations in the time range of seconds to tens of seconds[53]. The amplitude envelope of the alpha oscillations was extracted using the Hilbert transform applied to the FIR-filtered signals in the 8–13 Hz band. The analytical steps to quantify LRTC using DFA have been explained in detail previously[45,52]. Here, we used a standard assessment of the strength of LRTC on time scales from 2 to 20 seconds, which is reflected in the so-called "DFA exponent". An exponent of 0.5 characterizes an uncorrelated signal whereas an exponent in the interval of 0.5 to 1.0 indicate long-range temporal correlations with larger exponents indicating stronger correlations. in the alpha frequency band (8–13 Hz).

Excitation/inhibition ratio (fE/I)

The algorithm for estimating E/I ratio, was derived from the Critical Oscillations (CROS) model of ongoing neuronal activity[28], where a strong association is observed between the ratio of excitation/inhibition connectivity, oscillation amplitude, and LRTC. From these observations, a functional form of E/I ratio (*fE*/*I*) is estimated based on the Pearson correlation between the amplitude and LRTC within a signal. This method was validated using pharmacological manipulation in healthy subjects using a GABAergic drug (zolpidem), corroborating a reduction of *f*E/I ratios after the drug administration, and already tested in an ASD sample supporting the notion of large heterogeneity in E/I ratios (for details see Bruining *et al.*[27]). The analytical steps for the algorithm are as follows: to test the relationship between the amplitude and LRTC of the amplitude envelope of an oscillatory signal, it is necessary to have a measure of LRTC on short time-scales that is unbiased by the amplitude of the signal. To this end, an amplitude-normalized fluctuation function, $nF(t)$, is calculated

as follows: The signal is band-pass filtered (*i*), the amplitude envelope *A* extracted (*ii*), the signal profile, *S* can then be calculated as the cumulative sum of the demeaned amplitude envelope (*iii*),

$$S(t) = \sum_{k=1}^{t}(A(k) - \langle A \rangle) \qquad (1)$$

and split into windows of a certain size (the default used here is 5 seconds) in exactly the same way as during the DFA calculation[45,53]. As an additional step (*iv*), each of these signal-profile windows is divided by the mean of the amplitude envelope for that window calculated during step (*ii*). These amplitude-normalized windows are then detrended (*v*) and, subsequently, the normalized fluctuation function is calculated for each window as the standard deviation of the amplitude-normalized signal profile (*vi*). To calculate the functional excitation/inhibition ratio, *fE*/*I*, Pearson correlation between the amplitude and the normalized fluctuation function for the set of windows *W* (*vii*) is performed. *fE*/*I* is then defined as:

$$fE/I = 1 - r_{W_{amp}, W_{nF(t)}} \qquad (2)$$

Sub-critical (inhibition-dominated) networks will have an *fE*/*I* < 1, super-critical (excitation-dominated) networks *fE*/*I* > 1, and critical (E/I-balanced) networks will have *fE*/*I* = 1. A DFA > 0.6 inclusion criterion for networks or channels before computing the *fE*/*I* is used because networks without LRTC will not show a co-variation of amplitude and the fluctuation function. For our analyses, *fE*/*I* was calculated for windows of 5 seconds with 80% overlap.

Classification of EEG abnormalities

All recordings were visually inspected in windows of 10 seconds by a neurologist with training in clinical EEG (neurophysiology and epilepsy; EJM) and whom remained blind to the group label, and scored according to Luders & Noachtar's classification of EEG abnormalities[54]. When no abnormalities were detected, the EEG was classified as normal.

Statistical analysis

Two age categories were defined: children-adolescents (age 6–17 years) and adults (age 18–31 years). For both age groups, whole-brain average EEG biomarker values, as well as biomarker values over the 68 source-localized patches, were compared between the control groups (i.e., CON_C: control children-adolescents; CON_A: control adults) and the ASD groups

(i.e., ASD_C: children-adolescents with ASD; ASD_A: Adults with ASD). Finally, we investigated the correlation between EEG measures and clinical scores for the ASD groups.

Statistical analysis within EEG-abnormality subgroups

Participants with ASD were grouped based on the presence or absence of EEG abnormalities ($ASD_{C\text{-}qNL}$, $ASD_{C\text{-}qABN}$; $ASD_{A\text{-}qNL}$, $ASD_{A\text{-}qABN}$) and compared against the control groups and against each other (whole-brain average and per region). Additionally, we investigated the correlation between EEG measures in each subgroup and the clinical scores.

Non-specific EEG abnormalities can be present in the normal population. Although their clinical meaning is debated, they could be markers of common neurological conditions or unrecognized psychiatric disorders[55–58]. In this study we found EEG abnormalities in 9.8% of the subjects included in the control groups ($CON_{C\text{-}qABN}$, $CON_{A\text{-}qABN}$). To investigate if they showed distinct clinical and EEG characteristics, we compared them to controls with normal EEG ($CON_{C\text{-}qNL}$, $CON_{A\text{-}qNL}$), and also to the ASD_{qABN} subgroups. We also determined the difference between controls and ASD when no EEG abnormalities were present.

All patch-level comparisons were performed using Wilcoxon rank-sum test. For whole-brain analyses, we controlled for age, sex and IQ as covariates (ANCOVA test) and reported the adjusted *p*-values. Correlations between EEG measures and clinical scores were performed using partial (Pearson or Spearman) correlation coefficient, depending on whether normality assumptions were met, to additionally control for age, sex and IQ[59]. For patch-level analyses, False Discovery Rate (FDR, $q = 0.05$) was used to correct for multiple testing. Significance level was set at $p < 0.05$.

Results

503 participants aged 6–32 years old were recruited across five European specialist ASD centers and their EEG data collected as part of the EU-AIMS Longitudinal European Autism Project (LEAP)[33,34]. EEG recordings of 476 subjects were available. Given differences in EEG development throughout the lifespan[60–65], the data were divided into three age groups: children (6–11 years), adolescents (12–17 years), and adults (18–31 years). Due to the low sample sizes for the children and adolescents groups (**Figure 1**), and in order to simplify our analysis, we merged these into a single children-adolescents group (6–17 years) similar to

Bruining *et al.*[27]. After exclusion criteria and EEG preprocessing (**Figure 1**), the control groups comprised 91 children-adolescents (CON_{CA}, 7–17 years, M = 13.0 ± 3.0 years, 34 females) and 71 adults (CON_A, 18–31 years, M = 22.6 ± 3.6 years, 19 females). The ASD groups comprised 129 children-adolescents (ASD_{CA}, 6–17 years, M = 13.0 ± 3.0, 38 females) and 93 adults ($ASD_{A,}$ 18–30 years, M = 21.8 ± 3.2, 21 females). Demographic and main clinical characteristics of the sample included are described in **Table S1.** There was no difference in age between groups. As expected, the mean total IQ for the CON_C and CON_A was higher than the ASD_{CA} and ASD_A , respectively (CON_{CA}: M_{IQ} = 109.8 ± 1.4, ASD_{CA}: M_{IQ} = 98.3 ± 1.7, p <.0001; CON_A: M_{IQ} = 108 ± 1.4, ASD_A: M_{IQ} = 99.6 ± 1.9, p = .005) (**Table S1**).

In these EEG samples, we investigated the relative spectral power, long-range temporal correlations (LRTC, quantified by the DFA exponent), and functional excitation/inhibition ratio (fE/I) of alpha oscillations recorded with EEG during 2 minutes of eyes-closed rest.

ASD and controls exhibit similar variability of network-level E/I

First, we tested whether the current dataset replicates the previous finding of higher variability in ASD subjects compared to controls[27]. We did not observe significant EEG differences in mean or variance of alpha-band relative power, DFA exponent, or fE/I in either the children with ASD (ASD_{ch}) or adolescent groups (ASD_{ad}), at regional or at whole-brain level when compared to controls (**Figure S1, Table S2**). The lack of differential effects between children and adolescents in terms of alpha-band relative power, LRTC and fE/I, supported us merging these groups into one age group for greater statistical power in subsequent analyses (**Figure S2**). This age merge (children-adolescents, CA) did not change the results, and EEG differences remained non-significant for all compared biomarkers (**Figure 2**), both at patch and at whole-brain level (*relative power* (mean ± SEM): CON_{CA}= 0.33 ± 0.01, ASD_{CA}= 0.30 ± 0.01, p = 0.34, p_{Levene} = 0.28; *DFA*: CON_{CA}= 0.68 ± 0.01, ASD_{CA}= 0.67 ± 0.01, p = 0.52, p_{Levene} = 0.14; *fE/I*: CON_{CA}= 1.01 ± 0.02, ASD_{CA}= 0.99 ± 0.01, p = 0.26, p_{Levene} = 0.24).

Adults with ASD, however, showed wide-spread lower alpha-band relative power, and lower fE/I in frontal regions compared to controls (**Figure S2, Table S2)**. The lower fE/I in ASD adults was also significant at the whole-brain level (**Figure S2, Table S2**). Of note, neither of

the age groups with ASD presented with larger fE/I variance compared to controls in this sample.

Qualitative EEG abnormalities are associated with quantitative EEG differences in children-adolescents with ASD and controls

Following our previous observation that E/I variability may be related to qualitative EEG abnormalities[27], we graded the EEGs for qualitative abnormalities using the EEG classification of Lüders & Noachtar[54] (Methods), and investigated their association with spectral power, DFA exponents, and fE/I whilst being blinded to the group label and clinical characteristics of the participants.

In the children-adolescents group, we identified qualitative EEG abnormalities in 17% of the ASD_{CA} cases ($ASD_{CA\text{-}qABN,}$ n = 22), ranging from slowing of activity to epileptiform abnormalities. Of note, none of the subjects had a clinical history of seizures or had been diagnosed with epilepsy. We also found EEG abnormalities in 14% of the children-adolescents included in the CON_{CA} group (n = 13). In terms of clinical and demographical characteristics, children-adolescents with qualitative EEG abnormalities in both subgroups were significantly younger than those without abnormalities ($CON_{CA\text{-}qNL}$, M = 13.4 ± 2.9 years vs. $CON_{CA\text{-}qABN}$, M = 10.8 ± 2.5 years, p = .006; $ASD_{CA\text{-}qNL}$, M = 13.3 ± 2.9 years vs. $ASD_{CA\text{-}qABN}$, M = 11.5 ± 3.0 years; p = .006) (**Table S3**). While the presence or absence of qualitative EEG abnormalities did not have an impact on the clinical scales in children-adolescents with ASD, typically developing children-adolescents with qualitative EEG abnormalities showed a significantly higher VABS-composite and VABS-communication scores (**Table S3**).

In the adults group, we identified qualitative abnormalities in only 5% of the ASD_{A} cases ($ASD_{A\text{-}qABN}$, n = 5), and in 4% of the CON_{A} subjects ($CON_{A\text{-}qABN}$, n = 3). Due to the low numbers in the adults group, we could not investigate quantitative EEG differences between subgroups defined by qualitative EEG abnormalities.

Children-adolescents with ASD and abnormal EEG ($ASD_{CA\text{-}qABN}$, n = 22) had significantly lower alpha-band relative power, when compared to children-adolescents with normal EEG ($ASD_{CA\text{-}qNL}$, n = 107), in all but one patch (**Figure 3A**), and also at the whole-brain level (mean ± SEM: $ASD_{CA\text{-}qNL}$= 0.33 ± 0.01, $ASD_{CA\text{-}qABN}$= 0.18 ± 0.01, p < .0001, p_{Levene} =

0.028). fE/I was significantly lower in children with abnormal EEG, with the effects concentrated in the occipital region, but also present in the temporal, cingulate and frontal regions pertaining to the right hemisphere (**Figure 3C, Table S4**). A significant reduction in fE/I with abnormal EEG was also observed at the whole-brain level (mean ± SEM: $ASD_{CA\text{-}qNL}$ = 1.003 ± 0.014, $ASD_{CA\text{-}qABN}$ = 0.91 ± 0.031, p = 0.01, p_{Levene} = 0.66). No significant changes were observed in DFA (mean ± SEM: $ASD_{CA\text{-}qNL}$ = 0.67 ± 0.01, $ASD_{CA\text{-}qABN}$ = 0.67 ± 0.01, p = 0.90, p_{Levene} = 0.69). We also found significantly lower alpha-band relative power in the control children-adolescents with abnormal EEG ($CON_{CA\text{-}qABN}$, n = 13) compared to $CON_{CA\text{-}qNL}$ (n = 78, **Figure 3D**), both at patch and at whole brain-level (mean ± SEM: $CON_{CA\text{-}qNL}$= 0.35 ± 0.01, $CON_{CA\text{-}qABN}$= 0.17 ± 0.01, p < .0001, p_{Levene} = 0.005). fE/I in control-adolescents with abnormal EEG was lower at the whole-brain level (mean ± SEM: $CON_{CA\text{-}qNL}$ = 1.04 ± 0.02, $CON_{CA\text{-}qABN}$ = 0.86 ± 0.04, p = 0.0007, p_{Levene} = 0.55), was present in patches localized in the bilateral occipital regions, but also bilateral temporal and cingulate regions, right parietal and insular cortex as well as the left frontal region (**Figure 3F, Table S5**). No significant changes were observed in DFA (mean ± SEM: $CON_{CA\text{-}qNL}$ = 0.68 ± 0.01, $CON_{CA\text{-}qABN}$ = 0.68 ± 0.02, p = 0.60, p_{Levene} = 0.67). Notably, subjects with qualitative EEG abnormalities in the control ($CON_{CA\text{-}qABN}$) and ASD groups ($ASD_{CA\text{-}qABN}$) had comparable alpha-band relative power, DFA exponent, and fE/I (**Figure 4A-C**), as did subjects in the $ASD_{CA\text{-}qNL}$ and $CON_{CA\text{-}qNL}$ groups (**Figure 4D-F, Table S6**). No difference in DFA was observed between any of the groups **(Figure 3B,E, Figure 4B,E).**

Children-adolescent differences between abnormal and normal EEG are robust across studies

Given the similarity of the normal vs. abnormal EEG contrasts in children-adolescents with ASD and in controls (previous section, also **Figure 3**), we grouped all children-adolescents, regardless of the presence of ASD, to further investigate the quantitative differences between those with normal vs. abnormal EEG. We source-reconstructed EEG data from a previous study on ASD children-adolescents (SPACE-BAMBI)[27], and contrasted the biomarker values across abnormal and normal EEG. We found that the EU-AIMS and SPACE-BAMBI datasets show remarkably similar spatial contrasts patterns between normal and abnormal EEG (**Figure 5**), with both datasets showing significant patches predominantly in the right occipital, bilateral temporal and cingulate areas (**Table S7, S8**).

No relationship between clinical scales and EEG biomarkers

We expected that the modulation of EEG biomarkers by the presence of EEG abnormalities would reflect in their relationship with cognitive or behavioral scales. However, we did not find a significant correlation between our set of EEG biomarkers (patch or whole-brain level) and IQ, the Autism Diagnostic Observation Scale, Repetitive Behavior Scale-Revised, or with the Vineland-II Adaptive Behavior standard score for any of the groups (ASD or controls, even for those with qualitative EEG abnormalities) (**Table S9**; Pearson correlation, FDR multiple comparisons correction).

Discussion

The original hypothesis of E/I imbalances as a mechanism for ASD was partly based upon the observation of frequent EEG abnormalities—a hypothesis supported through diverse genetic, molecular and cellular studies[6,24,25,66–68] but lacking support from clinical measurements. Here, we tested the implication of EEG abnormalities on E/I balance using our fE/I measure in the EU-AIMS set of EEG recordings. Before evaluating for EEG abnormalities, we found no EEG differences and equal fE/I variability between cases and controls for the children-adolescents subsamples, while the adults with ASD showed lower fE/I and relative power in the alpha band, when compared to controls. After stratifying for qualitative EEG abnormalities, we found that both children-adolescents with and without ASD and an abnormal EEG associate with low relative power and low fE/I in the alpha band, which is our main finding. While relative power effects were widespread, low fE/I in subjects with abnormal EEG was found in localized patches. Notably, EEG abnormalities in the adult population were infrequent and, therefore, we could not corroborate this EEG phenotype in the adult cohort. Overall, our results show that EEG abnormalities concur with reduced alpha-band relative power and inhibition-dominated network dynamics, in agreement with our initial study of fE/I in clinical samples[27], and a finding we extend here by analyzing the alpha oscillations in source-reconstructed brain regions. Importantly, our findings support the notion that EEG abnormalities reflect a disturbance of E/I balance.

Our next challenge was to test whether EEG abnormalities have clinical implications or rather exist simultaneously or independently of pathology[69–71]. On average, we did not find

differences in IQ or clinical scores between ASD with or without EEG abnormalities, and we did not find significant correlations between network E/I and IQ or clinical questionnaires in either the ASD cohorts or controls, even after stratification for EEG abnormalities. Indeed, the E/I ratio of cortical networks determines network function, e.g., by modulating stimulus sensitivity and long-range functional connectivity[2,3], and specific spatial patterns of E/I imbalance are likely to result in different behavioral or cognitive deficits albeit not the ones measured with the clinical scales used in the present study, or the statistical power was insufficient. Another potential explanation is that the spectrum of ASD severity does not depend in a linear, straightforward manner, on factors that destabilize network functioning in terms of E/I balance. Furthermore, especially the lack of correlation between fE/I and clinical symptom scores in children-adolescents without EEG abnormalities may resonate with the broad clinical definition of the spectrum, in which many different mechanistic factors may contribute.

In fact, in the EU-AIMS study, the presence of EEG abnormalities was not constrained to the ASD sample, but could also be observed for controls. This could be explained by the plausible presence of other common neurological conditions in the EU-AIMS control sample, e.g., migraine, visual deficits, or subclinical psychiatric disorders[55,72] or the consequence of common medication (sleeping drugs, muscle relaxants, sedatives and antidepressants[73]. We acknowledge a more lenient inclusion criteria for the EU-AIMS control sample—which allowed for participants with different comorbidities to be enrolled and under some relevant psychotropic medication (e.g., melatonin, antidepressants and methylphenidate), which resulted in a heterogeneous “healthy” control sample. Although we accounted for this heterogeneity to the best of our knowledge by excluding data from participants in the control group reported to use psychotropic medication or with intellectual disability, it is still plausible that some conditions or medications were not explicitly registered and thus not controlled for. In line with this, we speculate that the primary mechanisms underlying the EEG abnormalities found in the control group would most likely differ from those found in ASD[55–58,74–78]. In fact, the type of EEG abnormalities were different between ASD and controls, e.g., epileptiform patterns were almost exclusive to ASD while the control group mainly showed altered background activity. However, it was not possible to investigate the different types of EEG abnormalities separately because of the small sample sizes and, thus, we ended with a broad definition of “an abnormal EEG” which is an important limitation. Detecting qualitative EEG abnormalities through an initial qualitative EEG inspection can

establish a more rigorous level of normative criteria beforehand, and can be used as a basis to enhance control samples[72].

The more lenient inclusion criteria for the EU-AIMS study might also explain the lack of increased variability in fE/I in ASD, compared to controls, which was originally reported in Bruining *et al.*[27]. On the other hand, these results are consistent with other recent EEG studies, which show similar fE/I variability of ASD and controls[79,80]. This, however, does not diminish the importance of association between fE/I and the presence of EEG abnormalities, which could be of potential value for pharmacological interventions targeting restoration of E/I balance.

The association between lower fE/I and qualitative EEG abnormalities was not globalized, but consistently localized in the occipital, temporal and cingulate regions, across both the ASD and CON groups, and was replicated across the EU-AIMS and SPACE-BAMBI datasets. Differences in activity in these regions have been associated with ASD and with sensory processing in particular[81–83]. In typically developing individuals who exhibited qualitative EEG abnormalities, lower fE/I in the same areas might be related to subclinical autistic traits[84]. Additionally, the wider spread of regions with lower fE/I, in typically developing children-adolescents, when compared with autistic individuals, could reflect a more heterogeneous set of factors contributing to the qualitative abnormalities and alterations in circuitry. Future studies should aim to determine the precise clinical impact of the presence of EEG abnormalities, in ASD and typically developing individuals, beyond conventional ASD questionnaires for instance using patient report outcome measures of sensory reactivity[85].

The lower fE/I for alpha oscillations observed in subjects with abnormal EEG is accompanied by decreased relative power in the same frequency band, which raises the question whether the fE/I reduction is a trivial effect of power shifts. However, fE/I is calculated from the correlation between windowed power and the temporal structure of amplitude fluctuations in alpha-band. Therefore, a change in fE/I could not occur only due to overall power shifts (e.g., doubling the alpha oscillation signal does not affect the correlation coefficient used to calculate fE/I), but requires a concomitant alteration in amplitude fluctuations, reflecting a different dynamical regime. Nonetheless, as has been investigated for DFA[86], a lower alpha-band power will lead to a decrease in the signal-to-noise ratio, which eventually will interfere with measuring the actual temporal structure. When this happens, both DFA and fE/I are expected to be underestimated and this could in principle have influenced our results. We do

not have a measure of signal-to-noise ratio to test this possibility; however, the absence of an effect of DFA speaks in favor of sufficient signal-to-noise ratio to adequately estimate the temporal structure and, thus, fE/I.

So, why are EEG abnormalities associated with lower fE/I? We previously studied two genetic disorders that are both strongly associated with ASD, epilepsy and intellectual disability, i.e., Tuberous Sclerosis Complex and STXBP1 syndrome[87,88]. In both disorders, patients showed reduced power and low fE/I ratios in most brain regions, when compared with healthy subjects. These findings seem counterintuitive, since epilepsy comorbidity and EEG abnormalities are traditionally considered a sign of cortical hyperexcitability. However, in an epileptogenic network, neuronal hyperexcitability can coexist with an excess of inhibition, e.g., both slowing of activity and increased localized network activity can be strong indicators of the epileptogenic zone interictally[89–92]. This interpretation would indicate a refinement of the initial E/I hypothesis in ASD and may be consistent with the notion that primary 'local' increases in E/I through genetic or metabolic defects, such as present in TSC or STXBP1, can trigger other compensatory inhibitory homeostatic mechanisms, e.g., synaptic scaling, lower presynaptic glutamate release and decrease postsynaptic AMPA receptor clustering or sensitivity[1,25,93]. At the network level, this may result in EEG abnormalities such as an increased slowing of activity—as it has been noted in both ASD and in the interictal period of epilepsy patients[27,49,94,95]. Furthermore, compensatory mechanisms may also account for so-called paradoxical effects that we and others observed when testing E/I-affecting drugs in ASD trials[32,96]. Together, the use of fE/I as a 'proxy marker' for E/I balance may help to link different neurobiological levels and reconsider oversimplistic extrapolation of cellular and local to global network-scale E/I interpretations. In clinical samples, stratification on the basis of EEG abnormalities and fE/I measurement may increase the power of studies on genetics of disease and on treatments targeting E/I balance.

CONCLUSION

The previously published association between EEG abnormalities and lower network level functional E/I ratio in the SPACE-BAMBI cohort is replicated in ASD and controls of the EU-AIMS LEAP sample. Source modeling found strong associations between the implicated anatomical regions in the two samples. Our findings indicate a method to stratify part of the neurophysiological heterogeneity of ASD and gain understanding of the effects of homeostatic interactions in E/I balance regulation.

Data availability

Due to privacy regulations of human subjects, we cannot provide the EEG files of the subjects included in our study. Analysis scripts to reproduce the figures and statistics, along with the underlying data, will be made available on figshare (https://figshare.com/), a website dedicated for sharing scientific data. The code for the fE/I algorithm is publicly available at https://github.com/rhardstone/fEI.

Acknowledgements

We thank all participants and their families for participating in this study. We also gratefully acknowledge the contributions of all members of the EU-AIMS LEAP group.

Funding

Netherlands Organization for Scientific Research (NWO) Physical Sciences Grant 612.001.123 (K.L.-H.)

Netherlands Organization for Scientific Research (NWO) Social Sciences 406-15-256 (A.-E.A.,K.L.-H.)

NWA-ORC Call (NWA.1160.18.200) (H.B., K.L.-H.).

NWO 'BRAINMODEL', project number 10250022110003 (2021-2027) (H.B., K.L.-H.)

EU H2020 'Human Brain Project' grant agreement no. 604102 (H.D.M.)

EU-AIMS (European Autism Interventions) and AIMS-2-TRIALS programmes which receive support from Innovative Medicines Initiative Joint Undertaking Grant No. 115300 and 777394, the resources of which are composed of financial contributions from the European Union's FP7 and Horizon2020 programmes, and from the European Federation of Pharmaceutical Industries and Associations (EFPIA) companies' in-kind contributions, and AUTISM SPEAKS, Autistica and SFARI; and by the Horizon2020 supported programme CANDY Grant No. 847818

Competing interests

H.B., K.L.-H., and S.-S.P. are shareholders of Aspect Neuroprofiles BV, which develops physiology-informed prognostic measures for neurodevelopmental disorders. K.L.-H. has filed the patent claim (PCT/NL2019/050167) “Method of determining brain activity”; with priority date 16 March 2018. TC has served as a paid consultant to F. Hoffmann-La Roche Ltd. and Servier; and has received royalties from Sage Publications and Guilford Publications. A.E.-A. is a paid consultant for Aspect Neuroprofiles BV. J.B. has been in the past 3 years a consultant to / member of advisory board of / and/or speaker for Takeda, Roche, Medice, Angelini, Neuraxpharm, and Servier. He is not an employee of any of these companies, and not a stock shareholder of any of these companies. He has no other financial or material support, including expert testimony, patents, royalties. P.G. and J.F.H. are full-time employees of F. Hoffmann - La Roche Ltd. T.B. served in an advisory or consultancy role for eye level, Infectopharm, Medice, Neurim Pharmaceuticals, Oberberg GmbH and Takeda. He received conference support or speaker’s fee by Janssen-Cilag, Medice and Takeda. He received royalities from Hogrefe, Kohlhammer, CIP Medien, Oxford University Press. The rest of the authors have no competing interests to declare. The funders of the study had no role in study design, data collection, data analysis, data interpretation, or writing of the report.

References

1. Turrigiano GG, Nelson SB. Homeostatic plasticity in the developing nervous system. *Nat Rev Neurosci*. 2004;5(2):97-107. doi:10.1038/nrn1327

2. Avramiea AE, Hardstone R, Lueckmann JM, B\’\im J, Mansvelder HD, Linkenkaer-Hansen K. Pre-stimulus phase and amplitude regulation of phase-locked responses are maximized in the critical state. *Elife*. 2020;9:e53016.

3. Avramiea AE, Masood A, Mansvelder HD, Linkenkaer-Hansen K. Long-Range Amplitude Coupling Is Optimized for Brain Networks That Function at Criticality. *J Neurosci*. 2022;42(11):2221-2233. doi:10.1523/JNEUROSCI.1095-21.2022

4. Kinouchi O, Copelli M. Optimal dynamical range of excitable networks at criticality. *Nat Phys*. 2006;2(5):348-351. doi:10.1038/nphys289

5. Ma Z, Turrigiano GG, Wessel R, Hengen KB. Cortical Circuit Dynamics Are Homeostatically Tuned to Criticality In Vivo. *Neuron*. 2019;104(4):655-664.e4. doi:10.1016/j.neuron.2019.08.031

6. Gogolla N, LeBlanc JJ, Quast KB, Südhof TC, Fagiolini M, Hensch TK. Common circuit defect of excitatory-inhibitory balance in mouse models of autism. *J Neurodev Disord*. 2009;1(2):172-181. doi:10.1007/s11689-009-9023-x

7. Baroncelli L, Braschi C, Spolidoro M, Begenisic T, Maffei L, Sale A. Brain Plasticity and Disease: A Matter of Inhibition. *Neural Plast*. 2011;2011:e286073. doi:10.1155/2011/286073

8. Fatemi SH, Halt AR, Stary JM, Kanodia R, Schulz SC, Realmuto GR. Glutamic acid decarboxylase 65 and 67 kDa proteins are reduced in autistic parietal and cerebellar cortices. *Biol Psychiatry*. 2002;52(8):805-810. doi:10.1016/S0006-3223(02)01430-0

9. Fatemi SH, Reutiman TJ, Folsom TD, Rooney RJ, Patel DH, Thuras PD. mRNA and Protein Levels for GABAAα4, α5, β1 and GABABR1 Receptors are Altered in Brains from Subjects with Autism. *J Autism Dev Disord*. 2010;40(6):743-750. doi:10.1007/s10803-009-0924-z

10. Oblak AL, Gibbs TT, Blatt GJ. Reduced GABAA receptors and benzodiazepine binding sites in the posterior cingulate cortex and fusiform gyrus in autism. *Brain Res*. 2011;1380:218-228. doi:10.1016/j.brainres.2010.09.021

11. Jamain S, Betancur C, Quach H, et al. Linkage and association of the glutamate receptor 6 gene with autism. *Mol Psychiatry*. 2002;7(3):302-310. doi:10.1038/sj.mp.4000979

12. Purcell AE, Jeon OH, Zimmerman AW, Blue ME, Pevsner J. Postmortem brain abnormalities of the glutamate neurotransmitter system in autism. *Neurology*. 2001;57(9):1618-1628. doi:10.1212/WNL.57.9.1618

13. He JL, Oeltzschner G, Mikkelsen M, et al. Region-specific elevations of glutamate + glutamine correlate with the sensory symptoms of autism spectrum disorders. *Transl Psychiatry*. 2021;11(1):1-10. doi:10.1038/s41398-021-01525-1

14. Horder J, Petrinovic MM, Mendez MA, et al. Glutamate and GABA in autism spectrum disorder—a translational magnetic resonance spectroscopy study in man and rodent models. *Transl Psychiatry*. 2018;8(1):1-11. doi:10.1038/s41398-018-0155-1

15. Hollestein V, Buitelaar JK, Brandeis D, et al. Developmental changes in fronto-striatal glutamate and their association with functioning during inhibitory control in autism spectrum disorder and obsessive compulsive disorder. *NeuroImage Clin*. 2021;30:102622. doi:10.1016/j.nicl.2021.102622

16. Ajram LA, Pereira AC, Durieux AMS, Velthius HE, Petrinovic MM, McAlonan GM. The contribution of [1H] magnetic resonance spectroscopy to the study of excitation-inhibition in autism. *Prog Neuropsychopharmacol Biol Psychiatry*. 2019;89:236-244. doi:10.1016/j.pnpbp.2018.09.010

17. Dickinson A, Jones M, Milne E. Measuring neural excitation and inhibition in autism: Different approaches, different findings and different interpretations. *Brain Res*. 2016;1648:277-289. doi:10.1016/j.brainres.2016.07.011

18. Sohal VS, Rubenstein JL. Excitation-inhibition balance as a framework for investigating mechanisms in neuropsychiatric disorders. *Mol Psychiatry*. 2019;24(9):1248-1257.

19. Parmeggiani A, Barcia G, Posar A, Raimondi E, Santucci M, Scaduto MC. Epilepsy and EEG paroxysmal abnormalities in autism spectrum disorders. *Brain Dev*. 2010;32(9):783-789. doi:10.1016/j.braindev.2010.07.003

20. Rubenstein JLR, Merzenich MM. Model of autism: increased ratio of excitation/inhibition in key neural systems. *Genes Brain Behav*. 2003;2(5):255-267. doi:10.1034/j.1601-183X.2003.00037.x

21. Boutros NN, Lajiness-O'Neill R, Zillgitt A, Richard AE, Bowyer SM. EEG changes associated with autistic spectrum disorders. *Neuropsychiatr Electrophysiol*. 2015;1(1):3. doi:10.1186/s40810-014-0001-5

22. Trauner DA. Behavioral correlates of epileptiform abnormalities in autism. *Epilepsy Behav*. 2015;47:163-166. doi:10.1016/j.yebeh.2014.10.020

23. Tang X, Jaenisch R, Sur M. The role of GABAergic signalling in neurodevelopmental disorders. *Nat Rev Neurosci*. 2021;22(5):290-307. doi:10.1038/s41583-021-00443-x

24. Lee E, Lee J, Kim E. Excitation/Inhibition Imbalance in Animal Models of Autism Spectrum Disorders. *Biol Psychiatry*. 2017;81(10):838-847. doi:10.1016/j.biopsych.2016.05.011

25. Nelson SB, Valakh V. Excitatory/Inhibitory Balance and Circuit Homeostasis in Autism Spectrum Disorders. *Neuron*. 2015;87(4):684-698. doi:10.1016/j.neuron.2015.07.033

26. Ahmad J, Ellis C, Leech R, et al. From mechanisms to markers: novel noninvasive EEG proxy markers of the neural excitation and inhibition system in humans. *Transl Psychiatry*. 2022;12(1):1-12. doi:10.1038/s41398-022-02218-z

27. Bruining H, Hardstone R, Juarez-Martinez EL, et al. Measurement of excitation-inhibition ratio in autism spectrum disorder using critical brain dynamics. *Sci Rep*. 2020;10(1):1-15.

28. Poil SS, Hardstone R, Mansvelder HD, Linkenkaer-Hansen K. Critical-state dynamics of avalanches and oscillations jointly emerge from balanced excitation/inhibition in neuronal networks. *J Neurosci Off J Soc Neurosci*. 2012;32(29):9817-9823. doi:10.1523/JNEUROSCI.5990-11.2012

29. Yizhar O, Fenno LE, Prigge M, et al. Neocortical excitation/inhibition balance in information processing and social dysfunction. *Nature*. 2011;477(7363):171-178. doi:10.1038/nature10360

30. van Vreeswijk C, Sompolinsky H. Chaos in Neuronal Networks with Balanced Excitatory and Inhibitory Activity. *Science*. 1996;274(5293):1724-1726. doi:10.1126/science.274.5293.1724

31. Carcea I, Froemke RC. Cortical plasticity, excitatory--inhibitory balance, and sensory perception. *Prog Brain Res*. 2013;207:65.

32. Juarez-Martinez EL, Sprengers JJ, Cristian G, et al. Prediction of Behavioral Improvement Through Resting-State Electroencephalography and Clinical Severity in a Randomized Controlled Trial Testing Bumetanide in Autism Spectrum Disorder. *Biol Psychiatry Cogn Neurosci Neuroimaging*. 2023;8(3):251-261. doi:10.1016/j.bpsc.2021.08.009

33. Charman T, Loth E, Tillmann J, et al. The EU-AIMS Longitudinal European Autism Project (LEAP): clinical characterisation. *Mol Autism*. 2017;8(1):27. doi:10.1186/s13229-017-0145-9

34. Loth E, Charman T, Mason L, et al. The EU-AIMS Longitudinal European Autism Project (LEAP): design and methodologies to identify and validate stratification biomarkers for autism spectrum disorders. *Mol Autism*. 2017;8(1):24. doi:10.1186/s13229-017-0146-8

35. Association AP, others. *Diagnostic and Statistical Manual of Mental Disorders (Text Revision)(DSM-IVTR). Washington, DC: American Psychiatric Association*.; 2000.

36. American Psychiatric Association D, Association AP, others. *Diagnostic and Statistical Manual of Mental Disorders: DSM-5*. Vol 5. American psychiatric association Washington, DC; 2013.

37. Organization WH. *The ICD-10 Classification of Mental and Behavioural Disorders: Diagnostic Criteria for Research*. World Health Organization; 1993.

38. Lord C, Rutter M, Dilavore PC, Risi S, Gotham K, Bishop S. Autism diagnostic observation schedule-Second edition (ADOS-2). *West Psychol Serv*. Published online 2012.

39. Lord C, Risi S, Lambrecht L, et al. The Autism Diagnostic Observation Schedule–Generic: A Standard Measure of Social and Communication Deficits Associated with the Spectrum of Autism.

40. Rutter M, Le Couteur A, Lord C, others. Autism diagnostic interview-revised. *Los Angel CA West Psychol Serv*. 2003;29(2003):30.

41. Constantino JN, Davis SA, Todd RD, et al. Validation of a Brief Quantitative Measure of Autistic Traits: Comparison of the Social Responsiveness Scale with the Autism Diagnostic Interview-Revised.

42. Lam KSL, Aman MG. The Repetitive Behavior Scale-Revised: Independent Validation in Individuals with Autism Spectrum Disorders. *J Autism Dev Disord*. 2007;37(5):855-866. doi:10.1007/s10803-006-0213-z

43. Sparrow SS, Cicchetti DV, Balla DA. *Vineland Adaptive Behavior Scales Vineland-II: Survey Forms Manual*. Pearson Minneapolis, MN; 2005.

44. Constantino J, Scale GSR. The Social Responsiveness Scale. *Los Angel CA West Psychol Serv*. Published online 2012.

45. Hardstone R, Poil SS, Schiavone G, et al. Detrended fluctuation analysis: a scale-free view on neuronal oscillations. *Front Physiol*. 2012;3(November):450. doi:10.3389/fphys.2012.00450

46. Fischl B. FreeSurfer. *Neuroimage*. 2012;62(2):774-781.

47. Klein A, Tourville J. 101 Labeled Brain Images and a Consistent Human Cortical Labeling Protocol. *Front Neurosci*. 2012;6. Accessed March 5, 2024. https://www.frontiersin.org/journals/neuroscience/articles/10.3389/fnins.2012.00171

48. Palva S, Palva JM. New vistas for α-frequency band oscillations. *Trends Neurosci*. 2007;30(4):150-158.

49. Wang J, Barstein J, Ethridge LE, Mosconi MW, Takarae Y, Sweeney JA. Resting state EEG abnormalities in autism spectrum disorders. *J Neurodev Disord*. 2013;5(1):24. doi:10.1186/1866-1955-5-24

50. Dickinson A, Varcin KJ, Sahin M, Nelson III CA, Jeste SS. Early patterns of functional brain development associated with autism spectrum disorder in tuberous sclerosis complex. *Autism Res*. 2019;12(12):1758-1773. doi:10.1002/aur.2193

51. Babadi B, Brown EN. A review of multitaper spectral analysis. *IEEE Trans Biomed Eng*. 2014;61(5):1555-1564.

52. Linkenkaer-Hansen K, Nikouline VV, Palva JM, Ilmoniemi RJ. Long-Range Temporal Correlations and Scaling Behavior in Human Brain Oscillations. *J Neurosci*. 2001;21(4):1370-1377.

53. Peng C K., Havlin S, Stanley HE, Goldberger AL. Quantification of scaling exponents and crossover phenomena in nonstationary heartbeat time series. *Chaos Interdiscip J Nonlinear Sci*. 1995;5(1):82-87. doi:10.1063/1.166141

54. Lüders H, Noachtar S. Atlas and classification of electroencephalography. *No Title*. Published online 2000.

55. Shelley BP, Trimble MR, Boutros NN. Electroencephalographic Cerebral Dysrhythmic Abnormalities in the Trinity of Nonepileptic General Population, Neuropsychiatric, and Neurobehavioral Disorders. *J Neuropsychiatry Clin Neurosci*. 2008;20(1):7-22. doi:10.1176/jnp.2008.20.1.7

56. Panayiotopoulos CP. The epilepsies: seizures, syndromes and management. Published online 2010.

57. Niedermeyer E, da Silva FL. *Electroencephalography: Basic Principles, Clinical Applications, and Related Fields*. Lippincott Williams & Wilkins; 2005.

58. Koutroumanidis M, Binnie CD, Elwes RDC, et al. Interictal regional slow activity in temporal lobe epilepsy correlates with lateral temporal hypometabolism as imaged with18FDG PET: neurophysiological and metabolic implications. *J Neurol Neurosurg Psychiatry*. 1998;65(2):170-176. doi:10.1136/jnnp.65.2.170

59. Conover WJ. *Practical Nonparametric Statistics*. Vol 350. john wiley & sons; 1999.

60. Gasser T, Verleger R, Bächer P, Sroka L. Development of the EEG of school-age children and adolescents. I. Analysis of band power. *Electroencephalogr Clin Neurophysiol*. 1988;69(2):91-99. doi:10.1016/0013-4694(88)90204-0

61. Chiang AKI, Rennie CJ, Robinson PA, van Albada SJ, Kerr CC. Age trends and sex differences of alpha rhythms including split alpha peaks. *Clin Neurophysiol*. 2011;122(8):1505-1517. doi:10.1016/j.clinph.2011.01.040

62. Schäfer CB, Morgan BR, Ye AX, Taylor MJ, Doesburg SM. Oscillations, networks, and their development: MEG connectivity changes with age. *Hum Brain Mapp*. 2014;35(10):5249-5261. doi:10.1002/hbm.22547

63. Somsen RJM, van't Klooster BJ, van der Molen MW, van Leeuwen HMP, Licht R. Growth spurts in brain maturation during middle childhood as indexed by EEG power spectra. *Biol Psychol*. 1997;44(3):187-209. doi:10.1016/S0301-0511(96)05218-0

64. Smit DJA, Geus EJC de, Nieuwenhuijzen ME van de, et al. Scale-Free Modulation of Resting-State Neuronal Oscillations Reflects Prolonged Brain Maturation in Humans. *J Neurosci*. 2011;31(37):13128-13136. doi:10.1523/JNEUROSCI.1678-11.2011

65. Neuhaus E, Lowry SJ, Santhosh M, et al. Resting state EEG in youth with ASD: age, sex, and relation to phenotype. *J Neurodev Disord*. 2021;13(1):33. doi:10.1186/s11689-021-09390-1

66. Satterstrom FK, Kosmicki JA, Wang J, et al. Large-Scale Exome Sequencing Study Implicates Both Developmental and Functional Changes in the Neurobiology of Autism. *Cell*. 2020;180(3):568-584.e23. doi:10.1016/j.cell.2019.12.036

67. Le Magueresse C, Monyer H. GABAergic Interneurons Shape the Functional Maturation of the Cortex. *Neuron*. 2013;77(3):388-405. doi:10.1016/j.neuron.2013.01.011

68. Levitt P, Eagleson KL, Powell EM. Regulation of neocortical interneuron development and the implications for neurodevelopmental disorders. *Trends Neurosci*. 2004;27(7):400-406. doi:10.1016/j.tins.2004.05.008

69. Nicotera AG, Hagerman RJ, Catania MV, et al. EEG Abnormalities as a Neurophysiological Biomarker of Severity in Autism Spectrum Disorder: A Pilot Cohort Study. *J Autism Dev Disord*. 2019;49(6):2337-2347. doi:10.1007/s10803-019-03908-2

70. Milovanovic M, Radivojevic V, Radosavljev-Kircanski J, et al. Epilepsy and interictal epileptiform activity in patients with autism spectrum disorders. *Epilepsy Behav*. 2019;92:45-52. doi:10.1016/j.yebeh.2018.12.011

71. Romero-González M, Navas-Sánchez P, Marín-Gámez E, et al. EEG abnormalities and clinical phenotypes in pre-school children with autism spectrum disorder. *Epilepsy Behav*. 2022;129:108619. doi:10.1016/j.yebeh.2022.108619

72. Boutros N, Mirolo HA, Struve F. Normative Data for the Unquantified EEG: Examination of Adequacy for Neuropsychiatric Research. *J Neuropsychiatry Clin Neurosci*. 2005;17(1):84-90. doi:10.1176/jnp.17.1.84

73. Blume WT. Drug effects on EEG. *J Clin Neurophysiol*. 2006;23(4):306-311.

74. De Curtis M, Avanzini G. Interictal spikes in focal epileptogenesis. *Prog Neurobiol*. 2001;63(5):541-567.

75. Arnal-Real C, Mahmoudzadeh M, Manoochehri M, Nourhashemi M, Wallois F. What triggers the interictal epileptic spike? A multimodal multiscale analysis of the dynamic of synaptic and non-synaptic neuronal and vascular compartments using electrical and optical measurements. *Front Neurol*. 2021;12:596926.

76. De Curtis M, Gnatkovsky V. Reevaluating the mechanisms of focal ictogenesis: the role of low-voltage fast activity. *Epilepsia*. 2009;50(12):2514-2525.

77. Stam CJ, Pritchard WS. Dynamics underlying rhythmic and non-rhythmic variants of abnormal, waking delta activity. *Int J Psychophysiol*. 1999;34(1):5-20.

78. Brigo F. Intermittent rhythmic delta activity patterns. *Epilepsy Behav*. 2011;20(2):254-256.

79. Li Q, Weiland RF, Konvalinka I, et al. Intellectually able adults with autism spectrum disorder show typical resting-state EEG activity. *Sci Rep*. 2022;12(1):19016.

80. Plueckebaum H, Meyer L, Beck AK, Menn KH. The developmental trajectory of functional excitation□inhibition balance relates to language abilities in autistic and allistic children. *Autism Res*. 2023;16(9):1681-1692.

81. Jassim N, Baron-Cohen S, Suckling J. Sensory Perception in Autism: An fMRI ALE Meta-Analysis. Published online April 2020. doi:10.31234/osf.io/p9n2z

82. Robertson CE, Baron-Cohen S. Sensory Perception in Autism. *Nat Rev Neurosci*. 2017;18(11):671-684. doi:10.1038/nrn.2017.112

83. Philip RCM, Dauvermann MR, Whalley HC, Baynham K, Lawrie SM, Stanfield AC. A Systematic Review and Meta-Analysis of the fMRI Investigation of Autism Spectrum Disorders. *Neurosci Biobehav Rev*. 2012;36(2):901-942. doi:10.1016/j.neubiorev.2011.10.008

84. Puzzo I, Cooper NR, Cantarella S, Fitzgerald PB, Russo R. The Effect of rTMS over the Inferior Parietal Lobule on EEG Sensorimotor Reactivity Differs According to Self-Reported Traits of Autism in Typically Developing Individuals. *Brain Res*. 2013;1541:33-41. doi:10.1016/j.brainres.2013.10.016

85. van Andel DM, van Stel HF, Scheepers FE, Oostrom KJ, Haverman L, Bruining H. The sensory-reactivity PROM set: identification of a parent reported outcome measure set for autism spectrum disorder. *J Patient-Rep Outcomes*. 2021;5:1-7.

86. Linkenkaer-Hansen K, Smit DJA, Barkil A, et al. Genetic contributions to long-range temporal correlations in ongoing oscillations. *J Neurosci*. 2007;27(50):13882-13889.

87. Houtman SJ, Lammertse HCA, van Berkel AA, et al. STXBP1 Syndrome Is Characterized by Inhibition-Dominated Dynamics of Resting-State EEG. *Front Physiol*. 2021;12. Accessed September 1, 2023. https://www.frontiersin.org/articles/10.3389/fphys.2021.775172

88. Juarez-Martinez EL, van Andel DM, Sprengers JJ, et al. Bumetanide Effects on Resting-State EEG in Tuberous Sclerosis Complex in Relation to Clinical Outcome: An Open-Label Study. *Front Neurosci*. 2022;16. Accessed March 5, 2024. https://www.frontiersin.org/journals/neuroscience/articles/10.3389/fnins.2022.879451

89. Nissen IA, Stam CJ, van Straaten ECW, et al. Localization of the Epileptogenic Zone Using Interictal MEG and Machine Learning in a Large Cohort of Drug-Resistant Epilepsy Patients. *Front Neurol*. 2018;9. Accessed March 5, 2024. https://www.frontiersin.org/journals/neurology/articles/10.3389/fneur.2018.00647

90. Englot DJ, Nagarajan SS, Wang DD, et al. The sensitivity and significance of lateralized interictal slow activity on magnetoencephalography in focal epilepsy. *Epilepsy Res*. 2016;121:21-28. doi:10.1016/j.eplepsyres.2016.01.009

91. Schönherr M, Stefan H, Hamer HM, Rössler K, Buchfelder M, Rampp S. The delta between postoperative seizure freedom and persistence: Automatically detected focal slow waves after epilepsy surgery. *NeuroImage Clin*. 2017;13:256-263. doi:10.1016/j.nicl.2016.12.001

92. Regional and global connectivity disturbances in focal epilepsy, related neurocognitive sequelae, and potential mechanistic underpinnings - Englot - 2016 - Epilepsia - Wiley Online Library. Accessed March 5, 2024. https://onlinelibrary.wiley.com/doi/full/10.1111/epi.13510

93. Turrigiano GG, Nelson SB. Hebb and homeostasis in neuronal plasticity. *Curr Opin Neurobiol*. 2000;10(3):358-364. doi:10.1016/S0959-4388(00)00091-X

94. Quraan MA, McCormick C, Cohn M, Valiante TA, McAndrews MP. Altered Resting State Brain Dynamics in Temporal Lobe Epilepsy Can Be Observed in Spectral Power, Functional Connectivity and Graph Theory Metrics. *PLOS ONE*. 2013;8(7):e68609. doi:10.1371/journal.pone.0068609

95. Terney D, Alving J, Skaarup CN, Wolf P, Beniczky S. The slow-wave component of the interictal epileptiform EEG discharges. *Epilepsy Res*. 2010;90(3):228-233. doi:10.1016/j.eplepsyres.2010.05.005

96. Ajram LA, Horder J, Mendez MA, et al. Shifting brain inhibitory balance and connectivity of the prefrontal cortex of adults with autism spectrum disorder. *Transl Psychiatry*. 2017;7(5):e1137-e1137. doi:10.1038/tp.2017.104

Figure legends

Figure 1. Flow diagram of the participants included for EEG analysis from the EU-AIMS Longitudinal European Autism Project (LEAP). A total of 503 subjects were screened for eligibility between January 2014 and March 2017 across five European specialist ASD centers. EEGs from 476 subjects were available. After preprocessing and exclusion criteria, 162 EEGs were included in the control group and 222 EEGs in the ASD group. All EEGs were cleaned, visually scored, and the following biomarkers were computed in the alpha-frequency band: relative power, Long-range temporal correlations (LRTC) quantified by detrended fluctuation analysis (DFA), and functional excitation-inhibition ratio (fE/I). Behavioral measures were available for the ASD group: Repetitive Behavior Scale-Revised (RBS-R); Vineland-II Adaptive Behavior standard scores (VABS); VABS Composite standard score (VABS-composite).

Figure 2. Alpha oscillations are quantitatively similar in the unstratified children-adolescents groups of ASD and controls. Grand-average flatmap representations of the two hemispheres, consisting of 68 patches (sources in the brain), are shown for CON_{CA} (*first column*) and ASD_{CA} (*second column*) for the alpha-band biomarkers. The grand-average difference plot of ASD_{CA}-CON_{CA} is shown in the small (*3rd column*), whereas the large plot represents significant differences after FDR correction as colored patches, and insignificant differences as gray patches (*4th column*). There were no significant differences in mean or variance of **(A)** relative power, **(B)** DFA, or **(C)** fE/I in the alpha band, between groups at the patch level (*4th column*) nor at the whole-brain level (*5th column*). Comparisons in boxplots (*5th column*) were based on the average value of the EEG biomarkers across all 68 patches (*p*-values are from ANCOVA / Levene's test of variability). Individual-subject values, mean, and SEM are shown for CON_{CA} (*blue circles*) and ASD_{CA} (*red circles*). For all comparisons at the whole-brain level, *p*-values are adjusted for age, IQ, and sex as covariates.

Figure 3. Children-adolescents with qualitative EEG abnormalities in both ASD and control groups show lower relative power and lower fE/I in the alpha-band, compared to those with normal EEG. Children-adolescents with ASD and abnormal EEG ($ASD_{CA-qABN}$) had lower alpha-band relative power **(A)** and lower fE/I mean **(C)** compared to ASD children-adolescents with normal EEG (ASD_{CA-qNL}). Interestingly, control children-adolescents with abnormal EEG ($CON_{CA-qABN}$) also showed lower relative alpha power **(D)** and lower fE/I **(F)** compared to controls with normal EEG (CON_{CA-qNL}) in similar brain

regions as the ASD group. No difference in DFA was observed between groups **(B, E)**. Relative alpha power exhibited a significantly narrower range of values both in the abnormal group of ASD and controls compared to the groups with qualitatively normal EEG (Levene's test) **(A, D)**. Grand-average flatmaps are shown for the cohort difference of the indicated comparisons (labels on top), where the small flatmaps represents the mean difference, and the large plot represents significant differences (*p*-value < 0.05, Wilcoxon rank-sum test, FDR corrected) as colored patches, and insignificant differences as gray patches. Comparisons in boxplots were based on the average value of the EEG biomarkers across all 68 patches (*p*-values are from ANCOVA / Levene's test of variability). Individual-subject values, mean, and SEM are shown for each comparison $ASD_{CA\text{-}qNL}/CON_{CA\text{-}qNL}$ (*blue circles*) and $ASD_{CA\text{-}qABN}/CON_{CA\text{-}qABN}$ (*red circles*). For all comparisons at the whole-brain level, *p*-values are adjusted for age, IQ, and sex as covariates.

Figure 4. Alpha oscillations are quantitatively similar when stratifying children-adolescents with ASD and controls by qualitative EEG abnormalities. EEG measures in control children-adolescents with qualitative EEG abnormalities ($CON_{CA\text{-}qABN}$) were not different from children-adolescents with ASD and abnormal EEG ($ASD_{CA\text{-}qABN}$) **(A-C)**. Moreover, measures in ASD children-adolescents with normal EEG ($ASD_{CA\text{-}qNL}$) were not different from controls with normal EEG ($CON_{CA\text{-}qNL}$) **(D-F)**. Grand-average flatmaps are shown for the cohort difference of the indicated comparisons (labels on top), where the small flatmaps represents the mean difference, and the large plot represents significant differences (*p*-value < 0.05, Wilcoxon rank-sum test, FDR corrected) as colored patches, and insignificant differences as gray patches. Comparisons in boxplots were based on the average value of the EEG biomarkers across all 68 patches (ANCOVA / Levene's test of variability). In the 3rd column, individual-subject values, mean, and SEM are shown for $CON_{CA\text{-}qABN}$ (*blue circles*) and $ASD_{CA\text{-}qABN}$ (*red circles*). In the 6th column, same values are shown for $CON_{CA\text{-}qNL}$ (*blue circles)*, and $ASD_{CA\text{-}qNL}$ (*red circles*). For all comparisons at the whole brain level, *p*-values are adjusted for age, IQ, and sex as covariates.

Figure 5. The distinction in alpha-band relative power and fE/I with respect to the presence/absence of qualitative abnormalities is robust across studies. After merging ASD and CON children-adolescent subjects that have qualitatively normal or abnormal EEG, respectively **(A-C)**, we observed very similar contrasts in alpha-band relative power and fE/I to those found in a re-analysis of the SPACE-BAMBI data previously published[27] **(D-F)**. Grand-average flatmaps are shown for the cohort difference of the indicated comparisons

(labels on top), where the small flatmaps represents the mean difference, and the large plot represents significant differences (p-value < 0.05, Wilcoxon rank-sum test, FDR corrected) as colored patches, and insignificant differences as gray patches. Comparisons in boxplots were based on the average value of the EEG biomarkers across all 68 patches (ANCOVA / Levene's test of variability). For all comparisons at the whole brain level, p-values are adjusted for age, IQ, and sex as covariates. In the 3rd and 6th column, *blue* and *red circles* represent individual-subject values, which are accompanied by the mean and SEM.

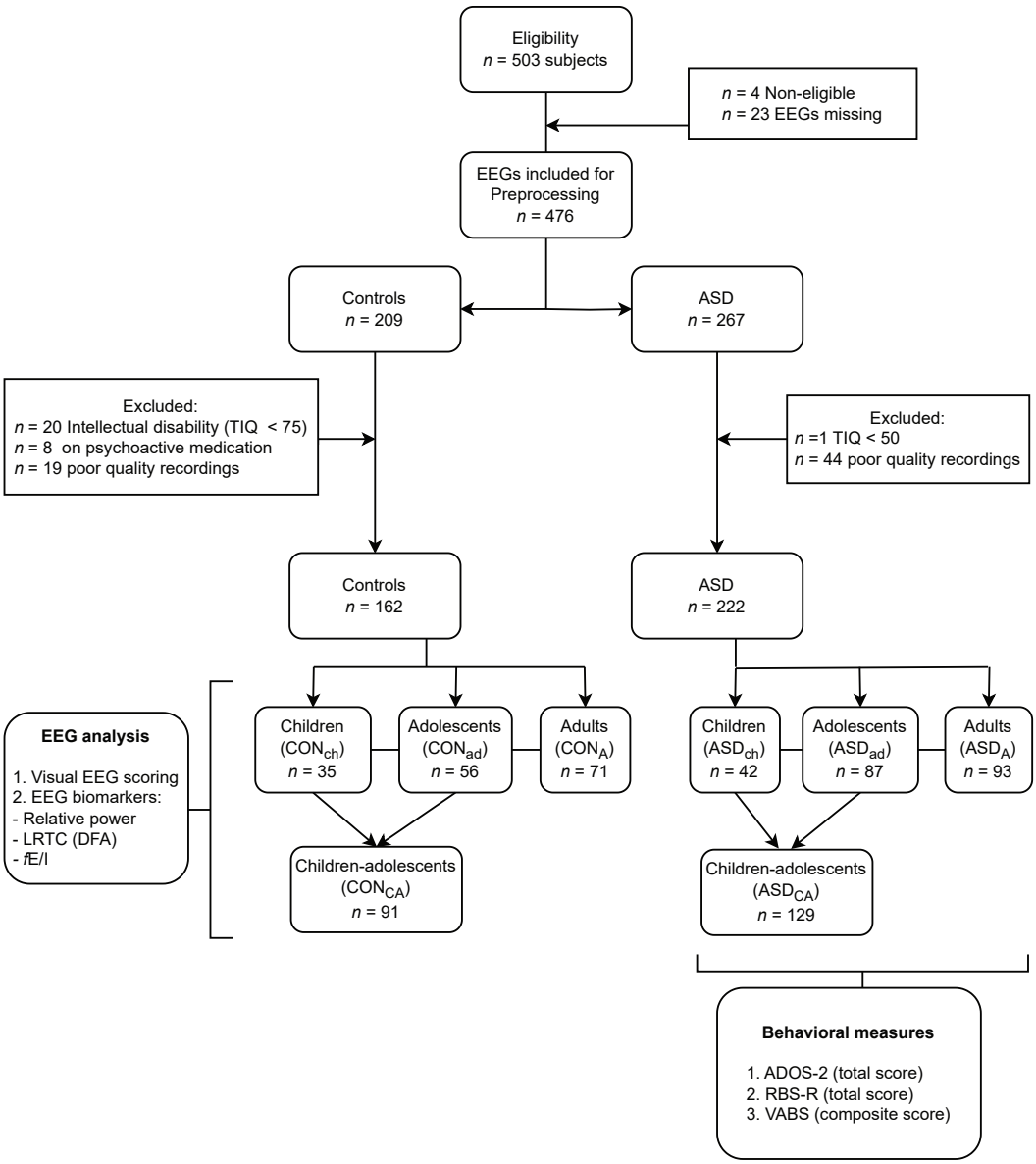

Figure 1. Flow diagram of the participants included for EEG analysis from the EU-AIMS Longitudinal European Autism Project (LEAP). A total of 503 subjects were screened for eligibility between January 2014 and March 2017 across five European specialist ASD centers. EEGs from 476 subjects were available. After preprocessing and exclusion criteria, 162 EEGs were included in the control group and 222 EEGs in the ASD group. All EEGs were cleaned, visually scored, and the following biomarkers were computed in the alpha-frequency band: relative power, Long-range temporal correlations (LRTC) quantified by detrended fluctuation analysis (DFA), and functional excitation-inhibition ratio (fE/I). Behavioral measures were available for the ASD group: Repetitive Behavior Scale-Revised (RBS-R); Vineland-II Adaptive Behavior standard scores (VABS); VABS Composite standard score (VABS-composite).

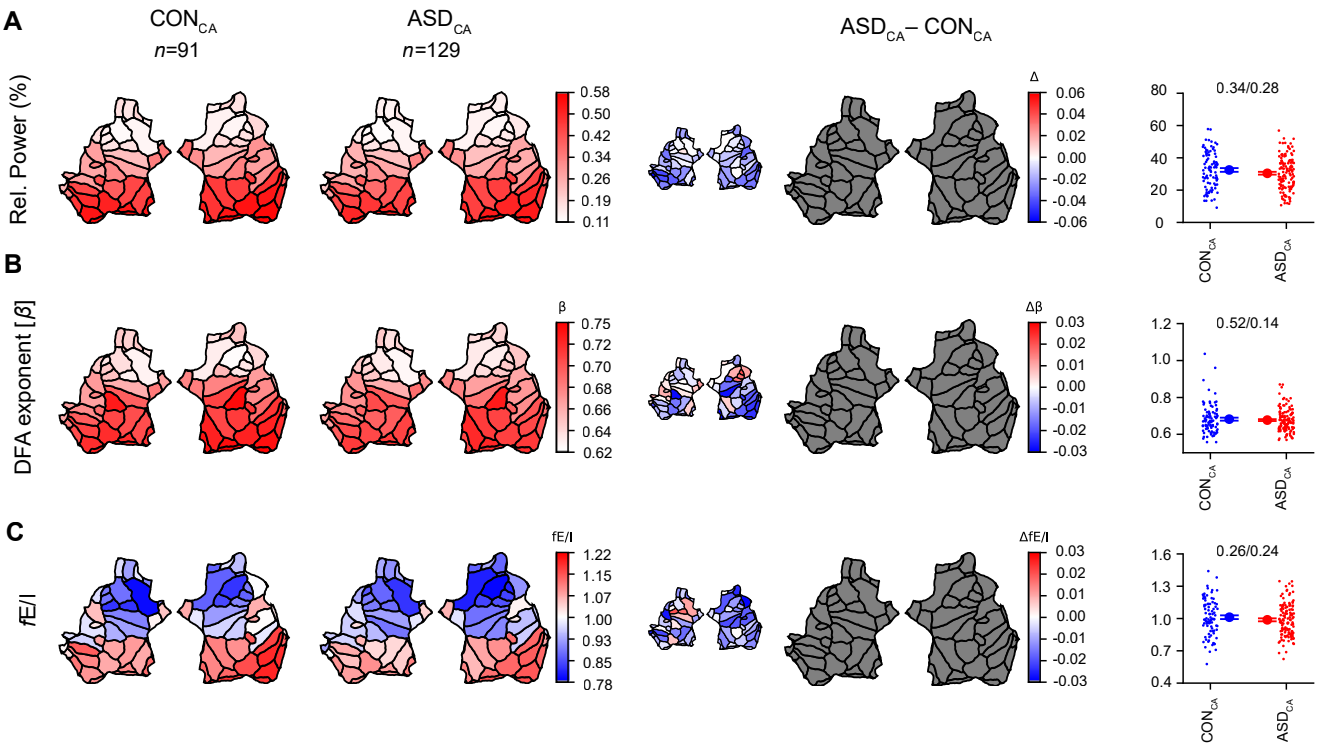

Figure 2. Alpha oscillations are quantitatively similar in the unstratified children-adolescents groups of ASD and controls. Grand-average flatmap representations of the two hemispheres, consisting of 68 patches (sources in the brain), are shown for CON_{CA} (*first column*) and ASD_{CA} (*second column*) for the alpha-band biomarkers. The grand-average difference plot of ASD_{CA}-CON_{CA} is shown in the small (*3rd column*), whereas the large plot represents significant differences after FDR correction as colored patches, and insignificant differences as gray patches (*4th column*). There were no significant differences in mean or variance of **(A)** relative power, **(B)** DFA, or **(C)** fE/I in the alpha band, between groups at the patch level (*4th column*) nor at the whole-brain level (*5th column*). Comparisons in boxplots (*5th column*) were based on the average value of the EEG biomarkers across all 68 patches (*p*-values are from ANCOVA / Levene's test of variability). Individual-subject values, mean, and SEM are shown for CON_{CA} (*blue circles*) and ASD_{CA} (*red circles*). For all comparisons at the whole-brain level, *p*-values are adjusted for age, IQ, and sex as covariates.

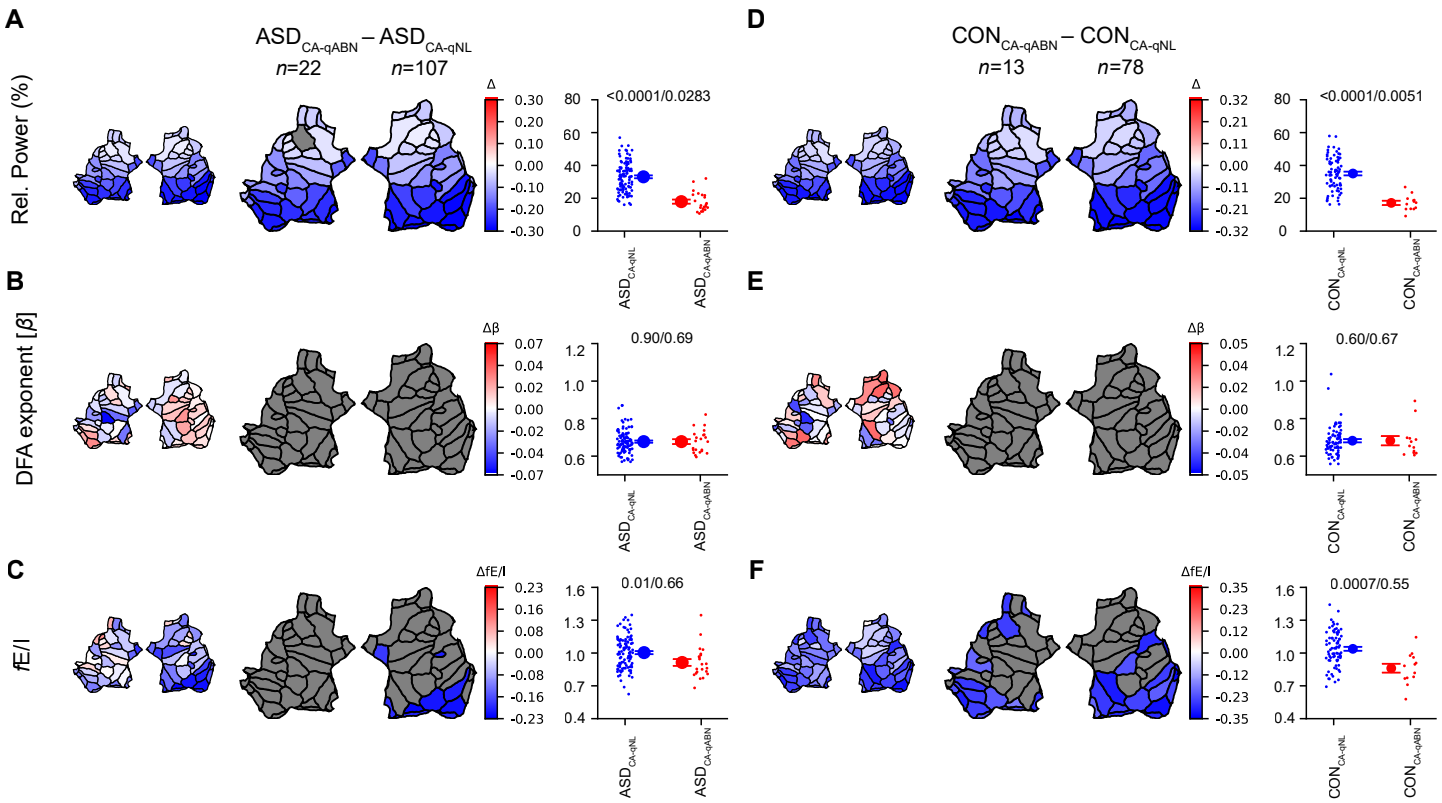

Figure 3. Children-adolescents with qualitative EEG abnormalities in both ASD and control groups show lower relative power and lower fE/I in the alpha-band, compared to those with normal EEG. Children-adolescents with ASD and abnormal EEG ($ASD_{CA-qABN}$) had lower alpha-band relative power **(A)** and lower fE/I mean **(C)** compared to ASD children-adolescents with normal EEG (ASD_{CA-qNL}). Interestingly, control children-adolescents with abnormal EEG ($CON_{CA-qABN}$) also showed lower relative alpha power **(D)** and lower fE/I **(F)** compared to controls with normal EEG (CON_{CA-qNL}) in similar brain regions as the ASD group. No difference in DFA was observed between groups **(B, E)**. Relative alpha power exhibited a significantly narrower range of values both in the abnormal group of ASD and controls compared to the groups with qualitatively normal EEG (Levene's test) **(A, D)**. Grand-average flatmaps are shown for the cohort difference of the indicated comparisons (labels on top), where the small flatmaps represents the mean difference, and the large plot represents significant differences (p-value < 0.05, Wilcoxon rank-sum test, FDR corrected) as colored patches, and insignificant differences as gray patches. Comparisons in boxplots were based on the average value of the EEG biomarkers across all 68 patches (p-values are from ANCOVA / Levene's test of variability). Individual-subject values, mean, and SEM are shown for ASD_{CA-qNL}/CON_{CA-qNL} (*blue circles*) and $ASD_{CA-qABN}$/$CON_{CA-qABN}$ (*red circles*). For all comparisons at the whole-brain level, p-values are adjusted for age, IQ, and sex as covariates.

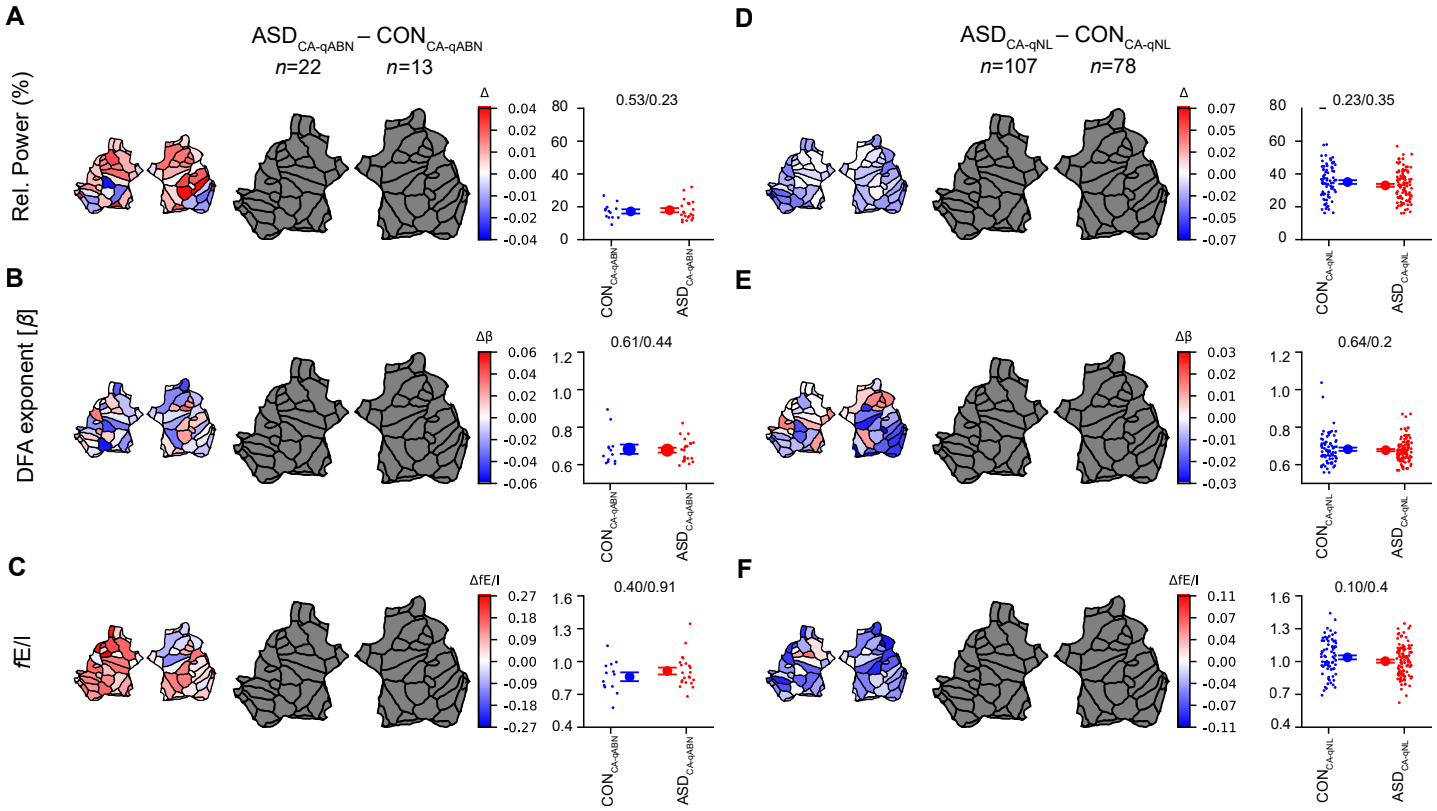

Figure 4. Alpha oscillations are quantitatively similar when stratifying children-adolescents with ASD and controls by qualitative EEG abnormalities. EEG measures in control children-adolescents with qualitative EEG abnormalities ($CON_{CA-qABN}$) were not different from children-adolescents with ASD and abnormal EEG ($ASD_{CA-qABN}$) **(A-C)**. Moreover, measures in ASD children-adolescents with normal EEG (ASD_{CA-qNL}) were not different from controls with normal EEG (CON_{CA-qNL}) **(D-F)**. Grand-average flatmaps are shown for the cohort difference of the indicated comparisons (labels on top), where the small flatmaps represents the mean difference, and the large plot represents significant differences (p-value < 0.05, Wilcoxon rank-sum test, FDR corrected) as colored patches, and insignificant differences as gray patches. Comparisons in boxplots were based on the average value of the EEG biomarkers across all 68 patches (ANCOVA / Levene's test of variability). In the 3rd column, individual-subject values, mean, and SEM are shown for $CON_{CA-qABN}$ (*blue circles*) and $ASD_{CA-qABN}$ (*red circles*). In the 6th column, same values are shown for CON_{CA-qNL} (*blue circles*), and ASD_{CA-qNL} (*red circles*). For all comparisons at the whole brain level, p-values are adjusted for age, IQ, and sex as covariates.

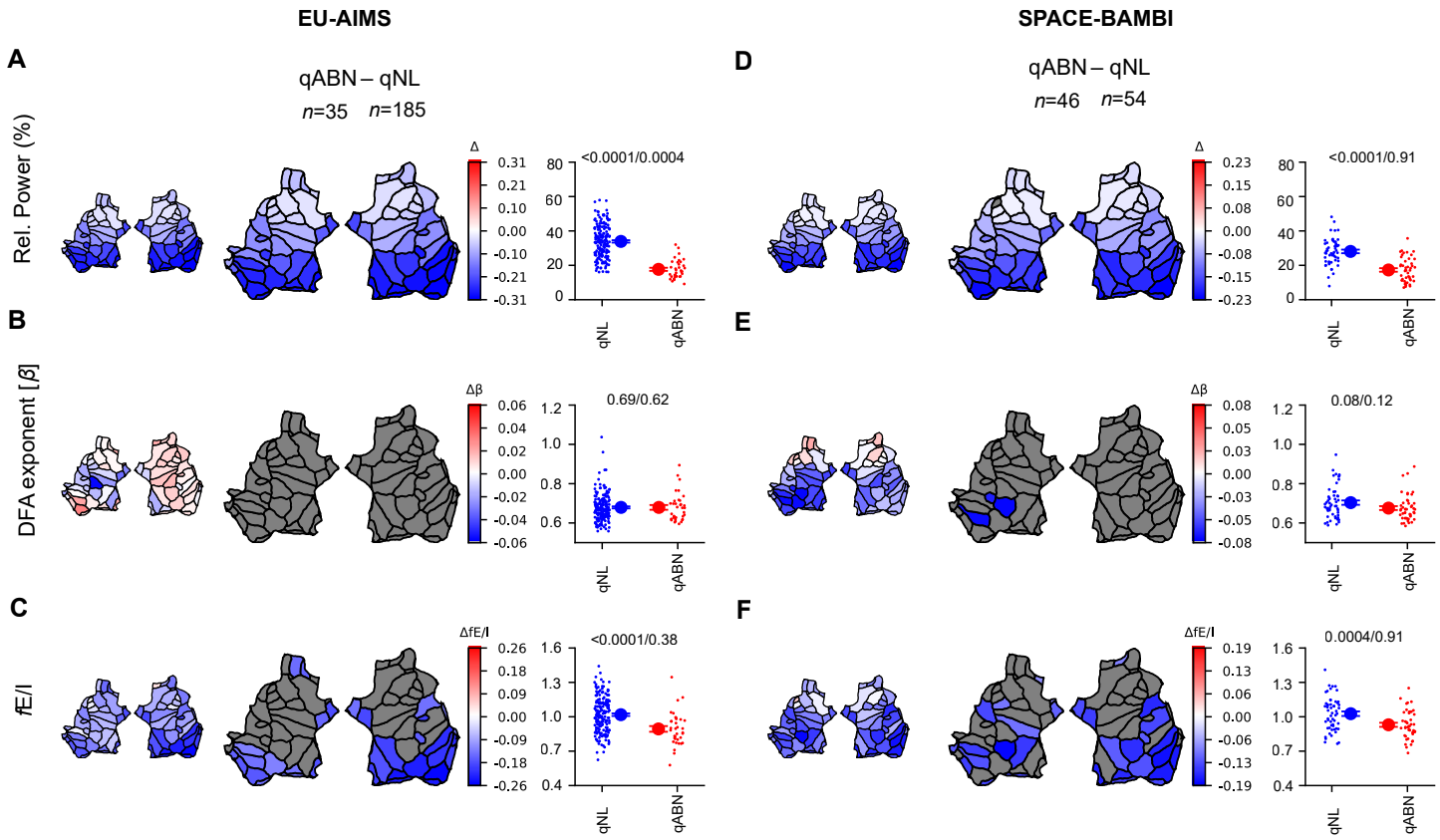

Figure 5. The distinction in alpha-band relative power and fE/I with respect to the presence/absence of qualitative abnormalities is robust across studies. After merging ASD and CON children-adolescent subjects that have qualitatively normal or abnormal EEG, respectively **(A-C)**, we observed very similar contrasts in alpha-band relative power and fE/I to those found in a re-analysis of the SPACE-BAMBI data previously published[27] **(D-F)**. Grand-average flatmaps are shown for the cohort difference of the indicated comparisons (labels on top), where the small flatmaps represents the mean difference, and the large plot represents significant differences (p-value < 0.05, Wilcoxon rank-sum test, FDR corrected) as colored patches, and insignificant differences as gray patches. Comparisons in boxplots were based on the average value of the EEG biomarkers across all 68 patches (ANCOVA / Levene's test of variability). For all comparisons at the whole brain level, p-values are adjusted for age, IQ, and sex as covariates. In the 3rd and 6th column, *blue* and *red circles* represent the individual-subject values, which are accompanied by the mean and SEM.